320 J. Med. Chem. 2011, 54, 320–330
DOI: 10.1021/jm101253v

Journal of Medicinal Chemistry Article

Phthalocyanine−Polyamine Conjugates as Highly Efficient Photosensitizers for Photodynamic Therapy

Xiong-Jie Jiang,[†] Sin-Lui Yeung,[‡] Pui-Chi Lo,*[,†] Wing-Ping Fong,*[,‡,§] and Dennis K. P. Ng*[,†,§]

[†]*Department of Chemistry,* [‡]*School of Life Sciences, and* [§]*Center of Novel Functional Molecules, The Chinese University of Hong Kong, Shatin, N.T., Hong Kong, China*

Received September 28, 2010

A series of silicon(IV) phthalocyanines substituted axially with different polyamine moieties have been prepared. Their fluorescence quantum yields (Φ_F = 0.03−0.08) in *N*,*N*-dimethylformamide are low because of reductive quenching by the amino moieties. The values are significantly increased in aqueous media (Φ_F = 0.12−0.21) as a result of protonation of the amino substituents. All the compounds are highly photocytotoxic against human colon adenocarcinoma HT29 cells and Chinese hamster ovary cells with IC_{50} values as low as 1.1 nM. Flow cytometric studies of two selected compounds (**2** and **5**) against HT29 cells have shown that they induce apoptosis extensively. As shown by confocal microscopy, these two compounds also show high affinity toward the lysosomes, but not the mitochondria, of the cells. Their in vivo photodynamic activity has also been investigated using HT29 tumor bearing nude mice. Both of them can effectively inhibit the growth of the tumor without causing apparent injury to the liver of the mice.

Introduction

Photodynamic therapy (PDT[a]) is a promising therapeutic modality for the treatment of a variety of premalignant and malignant diseases.[1−4] It utilizes the combined action of three individually nontoxic components, namely, a photosensitizer, light, and molecular oxygen, to cause cellular and tissue damage. Singlet oxygen generated through the photosensitization process is believed to be the major cytotoxic reactive oxygen species (ROS) responsible for the damage. Since the therapeutic outcome depends greatly on the behavior of the photosensitizers, including their selectivity toward malignant cells and efficiency in generating ROS, optimization of their photophysical and biological characteristics has been one of the major research focuses.[5−8] Over the past decade, various strategies have been explored to enhance the tumor selectivity of photosensitizers. These include encapsulation in liposomes,[9] polymeric micelles,[10,11] and silica-based nanoparticles[12] and bioconjugation to various tumor-specific vehicles such as epidermal growth factor, adenoviral proteins, and monoclonal antibodies.[13−15] Photodynamic molecular beacons that can be activated by tumor-associated proteases are also highly promising in this endeavor.[16,17]

Polyamines are naturally occurring compounds that play multifunctional roles in a number of cell processes including cell proliferation and differentiation.[18,19] Rapidly dividing cells such as tumor cells require a large amount of polyamines to sustain the rapid cell division. Part of these materials can be biosynthesized internally, while the majority is imported from exogenous sources through active and specific polyamine transporters (PAT).[20] These features have led to the use of polyamines as potent vectors for the selective delivery of chemotherapeutic and DNA-targeted drugs into cancer cells.[21,22] A substantial number of polyamine conjugates with cytotoxic drugs such as chlorambucil,[23,24] nitroimidazole,[25] aziridine,[26,27] acridine,[28] paclitaxel,[29] and camptothecin[30,31] have been reported. In most of the cases, their cytotoxicity and selectivity for tumor cells are enhanced. Several polyamine-appended porphyrin- and chlorin-based photosensitizers have also been prepared and studied very briefly for their in vitro photocytotoxicity.[32−36]

We have been interested in the development of efficient and selective photosensitizers for PDT with emphasis on the phthalocyanine derivatives.[37−40] Recently, we have reported a series of novel silicon(IV) phthalocyanines substituted with amino moieties.[41,42] These compounds exhibit remarkable pH-dependent properties showing enhanced fluorescence and singlet oxygen generation efficiency at lower pH in the range of 5−7. The results suggest that these compounds are promising pH-controlled and tumor-selective photosensitizers for PDT. In this paper, we extend the study to a series of related analogues that are substituted with a range of polyamines with different lengths and spacers between the nitrogen centers (compounds **1**−**9**, Figure 1). It is expected that the

*To whom correspondence should be addressed. For P.-C.L.: phone, (852) 2696 1326; fax, (852) 2603 5057; e-mail, pclo@cuhk.edu.hk. For W.-P.F.: phone, (852) 2609 6868; fax, (852) 2603 7246; e-mail, wpfong@cuhk.edu.hk. For D.K.P.N.: phone, (852) 2609 6375; fax, (852) 2603 5057; e-mail, dkpn@cuhk.edu.hk.

[a] Abbreviations: ALT, alanine aminotransferase; AST, aspartate aminotransferase; Boc, *tert*-butoxycarbonyl; CHO, Chinese hamster ovary; DFMO, α-difluoromethylornithine; DMEM, Dulbecco's modified Eagle's medium; DMF, *N*,*N*-dimethylformamide; DPBF, 1,3-diphenylisobenzofuran; EI, electron impact; ESI, electrospray ionization; FAB, fast atom bombardment; GFP, green fluorescent protein; OMs, methanesulfonate; PAT, polyamine transporters; PBS, phosphate buffered saline; PDT, photodynamic therapy; PET, photoinduced electron transfer; PI, propidium iodide; ROS, reactive oxygen species; SEM, standard error of the mean; THF, tetrahydrofuran; ZnPc, zinc(II) phthalocyanine; Φ_F, fluorescence quantum yield; Φ_Δ, singlet oxygen quantum yield; IC_{50}, dye concentration required to kill 50% of the cells.

 Published on Web 12/07/2010

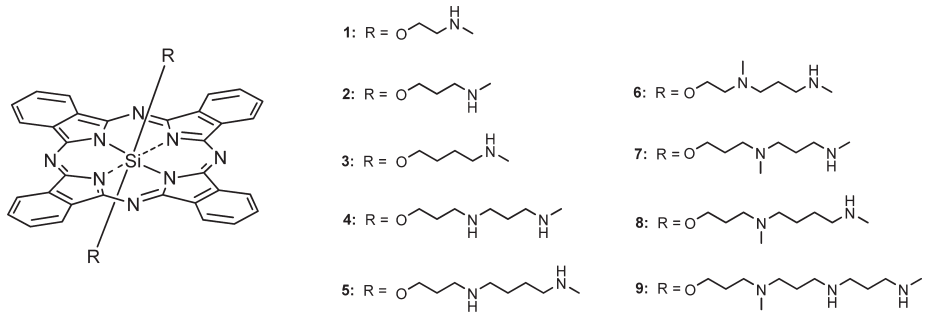

Figure 1. Structures of phthalocyanines **1**−**9**.

polyamine moieties, which are protonated under physiological conditions, can enhance the hydrophilicity and reduce the aggregation tendency of the phthalocyanine core and more importantly can enhance the cellular uptake of the dyes, resulting in higher photodynamic activities. We report herein the synthesis, basic photophysical properties, and the in vitro and in vivo studies of these phthalocyanine−polyamine conjugates.

Results and Discussion

Synthesis and Characterization. The synthesis of various polyamine derivatives has been well documented,[43] which forms the basis of our synthetic strategies for these conjugates. Scheme 1 shows the synthetic route of the precursors **17**−**19**. Treatment of the commercially available hydroxyamines **10**−**12** with *tert*-butoxycarbonyl (Boc) protected methanesulfonate **13** in acetonitrile gave the substituted products **14**−**16**. The Boc group of these compounds was removed by the treatment with hydrochloric acid. After neutralization, the hydroxyamines **17**−**19** were obtained in good yields. Similarly, the hydroxyamines **24** and **25** were prepared according to the route shown in Scheme 2. Treatment of compound **20** with methanesulfonyl chloride and triethylamine gave compound **21**, which then underwent mesylate displacement reactions with **10** and **12** to afford **22** and **23**, respectively. Subsequent *N*-Boc deprotection of these compounds gave hydroxyamines **24** and **25** in satisfactory yields.

Hydroxyamine **29**, having the longest chain length among the polyamines being studied, was prepared using a similar procedure (Scheme 3). By use of Boc-protected hydroxyamine **14** as a starting material, *N*-Boc protection of the internal amino group followed by *O*-sulfonylation afforded compound **27**. Substitution reaction of this compound with hydroxyamine **12** followed by *N*-Boc deprotection with acid gave hydroxyamine **29**.

Silicon(IV) phthalocyanines are excellent candidates as second-generation photosensitizers for PDT.[37,38,40−42] The silicon center can impart desirable photophysical properties to the macrocycles and allow the introduction of appropriate axial ligands to adjust their amphiphilicity, reduce their aggregation tendency, and enhance their tumor selectivity. We therefore conjugated various polyamine moieties to a silicon(IV) phthalocyanine core. Compounds **1**−**9** were prepared readily by ligand substitution reactions of silicon(IV) phthalocyanine dichloride with hydroxyamines **11**, **12**, **17**−**19**, **24**, **25**, and **29** and 4-(methylamino)-1-butanol (**30**) in the presence of pyridine in toluene. The products were purified by recrystallization from a mixture of $CHCl_3$ and 1-hexane (1:4 v/v). All new compounds were characterized with various spectroscopic methods and elemental analyses (for phthalocyanines **1**−**9**) or accurate mass measurements (for the precursors).

Electronic Absorption and Photophysical Properties. The electronic absorption and basic photophysical data for **1**−**9** measured in *N*,*N*-dimethylformamide (DMF) are summarized in Table 1. All the compounds gave typical absorption spectra of nonaggregated phthalocyanines, showing the B-band at 354−356 nm, Q-band at 672−674 nm, together with two vibronic bands at 604−607 and 643−647 nm. The very similar Q-band absorptions indicate that the macrocyclic π system is not perturbed by the axial ligands. Figure 2 shows the UV−vis spectra of **1** in DMF at various concentrations given as an example. The very sharp Q-band, which strictly follows the Lambert−Beer law, suggests that aggregation is not significant for this compound. Upon excitation at 610 nm, these compounds showed a weak fluorescence emission at 676−678 nm with a fluorescence quantum yield (Φ_F) of 0.03−0.08 relative to unsubstituted zinc(II) phthalocyanine (ZnPc) ($\Phi_F = 0.28$).[44] The weak fluorescence may be attributed to the quenching of the singlet excited state of the phthalocyanine core by the axial amino moieties through intramolecular photoinduced electron transfer (PET).[41,42,45]

To evaluate the photosensitizing efficiency of these compounds, their singlet oxygen quantum yields (Φ_Δ) were determined by a steady-state method using 1,3-diphenylisobenzofuran (DPBF) as the scavenger. The concentration of the quencher was monitored spectroscopically at 414 nm with time of irradiation (Figure S1 in the Supporting Information), from which the values of Φ_Δ could be determined. As shown in Table 1, all of the phthalocyanines **1**−**9** can generate singlet oxygen in DMF but not in an effective manner. The values of Φ_Δ are only 0.03 to 0.15 relative to ZnPc ($\Phi_\Delta = 0.56$).[46] The low singlet oxygen generation efficiency may also be attributed to the PET process.[41,42,45]

Compounds **1**−**9** are quite soluble in water because the amino groups are protonated under this condition. Their electronic absorption and fluorescence spectra were also recorded in water in the presence of a trace amount of organic solvents [0.1% tetrahydrofuran (THF) (for **1**−**3**) or 0.1% MeOH (for **4**−**9**)]. The data are compiled in Table S1 (Supporting Information). All the compounds showed similar spectral features except for compound **1**, which gave a less intense Q-band (see the absorption spectra of **1** and **2** in Figure S2 in the Supporting Information), suggesting that it is more aggregated than the other analogues. The Q bands were all red-shifted by ∼10 nm compared with those recorded in DMF. Upon excitation at 610 nm, these compounds showed a fluorescence emission at 687−688 nm with a fluorescence quantum yield of 0.12−0.21. The values are significantly higher than those measured in DMF (Table 1). It is likely that the

amino moieties are protonated in the aqueous environment, resulting in inhibition of the PET process.

The absorption and emission spectra of compounds **1**−**9** were also measured in citrate buffer solutions with different pH. All the compounds, except **1**, gave very similar absorption spectra showing that they are essentially nonaggregated under an acidic or neutral condition (pH < 8). Compound **1** gave a less intense Q-band and exhibited a higher aggregation tendency. The variation of the Q-band absorbance at 683 nm with the pH value for all these compounds is shown in Figure S3 (Supporting Information). It can be seen that there is no significant change in the absorbance when the pH increases from 5 to 8. The change in fluorescence intensity with pH for all these compounds is depicted in Figure S4 (Supporting Information). In general, the fluorescence intensity increased as the pH decreased. Among these compounds, phthalocyanine **6** showed the most distinct change. Its fluorescence intensity increased by about 4-fold when the pH changed from 9 to 6 (Figure 3). It is believed that the amino groups of **6** are fully protonated at lower pH, which greatly reduces the aggregation and inhibits the intramolecular PET process, resulting in a stronger fluorescence emission.[41,42]

In Vitro Studies. The photodynamic activities of phthalocyanines **1**−**9** were first evaluated against two different cell lines, namely, human colon adenocarcinoma HT29 and Chinese hamster ovary (CHO) cells. The former is often used in our studies,[37−42,45] while the latter is known to have high PAT activity.[47] Figure 4 shows the effects of **2** on both the cell lines given for exemplification. This compound is essentially noncytotoxic in the absence of light but exhibits high photocytotoxicity, particularly for the HT29 cells. All the compounds show similar survival curves, and their IC_{50} values are compiled in Table 2. Interestingly, most of them show higher photocytotoxicity toward the HT29 cells. Compounds **2** and **3**, in particular, exhibit the highest potency and selectivity. Their IC_{50} values for the HT29 cells (1.1 and 1.4 nM, respectively) are about 30-fold lower than those for the CHO cells (35.0 and 33.1 nM, respectively). Their photocytotoxicity is much higher than that of the classical photosensitizer porfimer sodium ($IC_{50} \sim 4.5$ μg mL^{-1} under the

Scheme 1. Synthesis of Hydroxyamines **17**−**19**

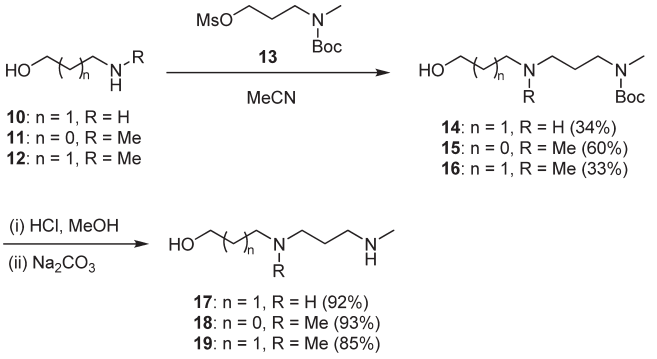

Scheme 2. Synthesis of Hydroxyamines **24** and **25**

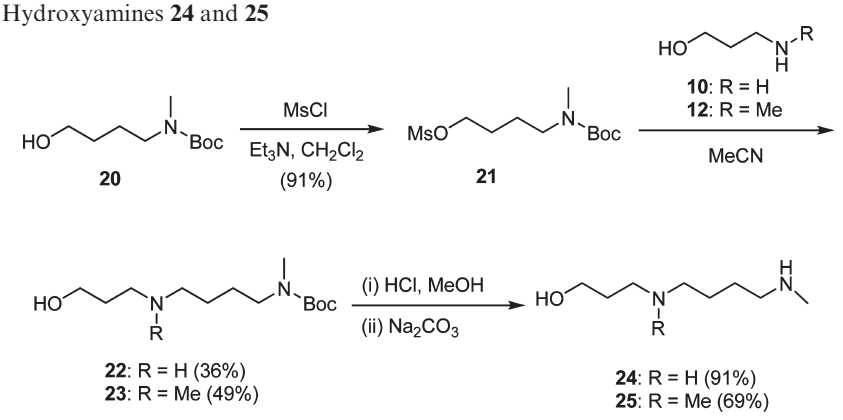

Scheme 3. Synthesis of Hydroxyamine **29**

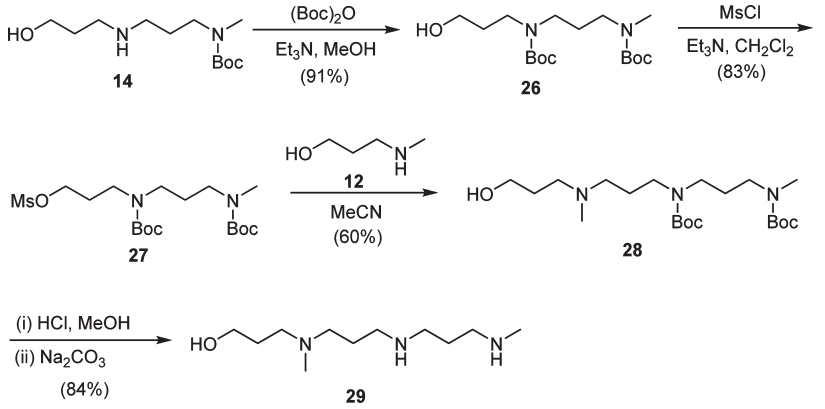

Table 1. Electronic Absorption and Photophysical Data for **1**−**9** in DMF

compd	λ_{max} (nm) (log ε)	λ_{em} (nm)[a]	Φ_F[b]	Φ_Δ[c]
1	354 (4.81), 604 (4.55), 643 (4.48), 672 (5.35)	676	0.03	0.06
2	354 (4.85), 606 (4.58), 644 (4.50), 673 (5.38)	678	0.05	0.13
3	356 (4.77), 606 (4.51), 644 (4.45), 673 (5.31)	677	0.07	0.15
4	354 (4.78), 606 (4.52), 644 (4.45), 673 (5.32)	677	0.06	0.09
5	356 (4.85), 606 (4.57), 644 (4.50), 673 (5.37)	677	0.04	0.13
6	356 (4.86), 607 (4.57), 647 (4.51), 674 (5.37)	677	0.07	0.14
7	354 (4.85), 606 (4.59), 644 (4.52), 674 (5.39)	678	0.08	0.13
8	356 (4.83), 606 (4.55), 644 (4.48), 673 (5.34)	677	0.04	0.06
9	354 (4.82), 606 (4.56), 644 (4.49), 673 (5.35)	677	0.03	0.03

[a] Excited at 610 nm. [b] Using ZnPc in DMF as the reference [fluorescence quantum yield (Φ_F) = 0.28]. [c] Using ZnPc as the reference [singlet oxygen quantum yield (Φ_Δ) = 0.56 in DMF].

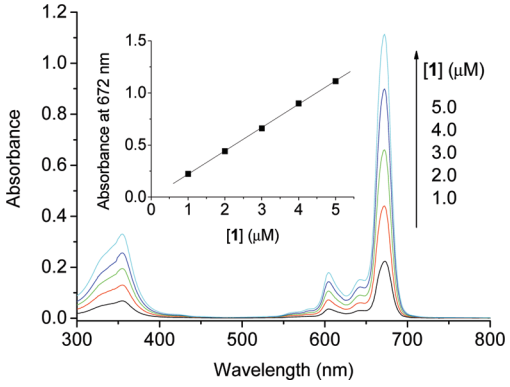

Figure 2. UV−vis spectra of **1** in DMF at different concentrations. The inset plots the Q-band absorbance at 672 nm versus the concentration of **1**.

same experimental conditions versus 0.8−1.0 ng mL^{-1} for **2** and **3** against HT29) and pheophorbide *a* (IC_{50} = 0.5 μM for HT29).[48] In fact, they represent the most potent photosensitizers developed in our laboratory so far.[37−42,45] A longer polyamine chain does not enhance the in vitro photocytotoxicity.

For the light source that we used (halogen lamp, λ > 610 nm), only a narrow region of the light (at about 610−700 nm) is absorbed by the compounds to initiate the photodynamic action. Therefore, the actual total fluence required should be lower than 48 J cm^{-2}. To study the effect of light dose, the cytotoxicity of **2** on HT29 cells was also evaluated upon illumination with a diode laser at 675 nm. It was found that a total fluence of 16 J cm^{-2} (power of 0.2 W) is sufficient to attain a similar effect (IC_{50} ~ 1 nM) (Figure 5). By reduction of the total fluence to 4 J cm^{-2}, the photoactivity was lower, giving an IC_{50} value of ~16 nM.

To have a better understanding on the role of the polyamine moieties, we performed some additional experiments. First, during the incubation of HT29 and CHO cells with **5** and **8** (up to 1 μM), a solution of spermidine in the culture medium (1 mM) was added. In addition to this competitive study, we also examined the effect of α-difluoromethylornithine (DFMO). This is a well-studied mechanism-based inhibitor of ornithine decarboxylase, which is the rate-limiting enzyme in polyamine biosynthesis from L-ornithine.[49,50] It can induce an up-regulation of the PAT activity of the tumor cells, thereby potentially promoting the uptake of polyamine conjugates. In this study, CHO cells were incubated with **5**, **8**, and **9** (up to 0.25 μM), respectively, in the presence of DFMO (5 mM). However, for all these experiments, the effects of spermidine and DFMO were insignificant,

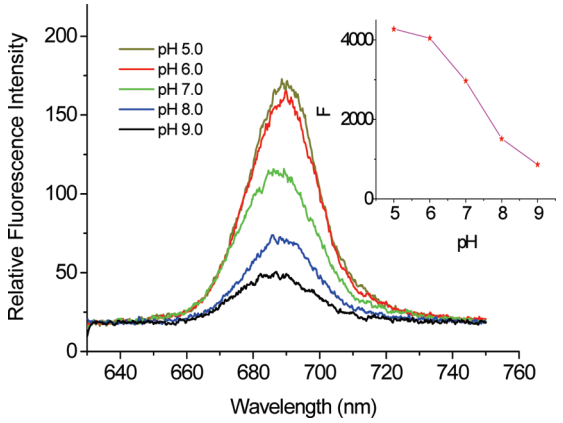

Figure 3. Fluorescence spectra of **6** (2 μM) in citrate buffer solutions with different pH (excited at 610 nm). The inset shows the variation of the relative fluorescence intensity (*F*) with pH.

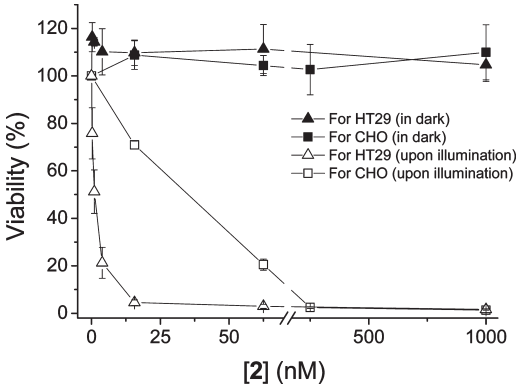

Figure 4. Comparison of the cytotoxic effects of **2** on HT29 and CHO cells in the absence and presence of light (λ > 610 nm, 40 mW cm^{-2}, 48 J cm^{-2}). Data are expressed as mean values ± standard error of the mean (SEM) of three independent experiments, each performed in quadruplicate.

Table 2. Comparison of the IC_{50} Values of Phthalocyanines **1**−**9** against HT29 and CHO Cells

	IC_{50} (nM)	
compd	HT29	CHO
1	11.4	61.9
2	1.1	35.0
3	1.4	33.1
4	5.5	29.0
5	31.3	25.8
6	21.7	36.5
7	8.8	15.6
8	23.4	21.3
9	22.8	46.2

suggesting that the cellular uptake of these phthalocyanines may not involve the PAT of the cells.

It has been reported that PDT is a strong inducer of apoptosis in many situations.[51] The earliest hallmark of apoptosis is the loss of plasma membrane asymmetry. In apoptotic cells, the membrane phospholipid phosphatidylserine is translocated from the inner to outer leaflet of the plasma membrane, thus exposing phosphatidylserine to the external cellular environment. Annexin V green fluorescent protein (GFP) has high affinity for phosphatidylserine and therefore serves as a sensitive probe for identifying apoptotic cells.[52] Generally, annexin V-GFP is costained together with

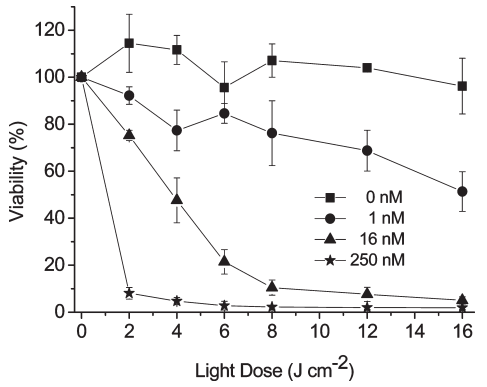

Figure 5. Light dose dependent photocytotoxicity of **2** against HT29 cells. The cells were illuminated with a diode laser at 675 nm. Data are expressed as mean values ± SEM of three independent experiments, each performed in quadruplicate.

propidium iodide (PI), which is a fluorescent probe to distinguish viable cells from dead cells, as the former with intact membranes exclude PI. We studied the cell death mechanism induced by phthalocyanines **2** and **5** by examining the dual fluorescence of annexin V-GFP/PI using flow cytometry. The cell populations at different phases of cell death, namely, viable (annexin V-GFP$^-$/PI$^-$), early apoptotic (annexin V-GFP$^+$/PI$^-$), and necrotic or late-stage apoptotic (annexin V-GFP$^+$/PI$^+$), were examined at different drug doses. Figure 6 shows the flow cytometric analysis for compound **2** after PDT treatment on HT29 cells. It can be seen that most of the cells are negative for annexin V-GFP and PI after the treatment with **2** (16 nM) in the absence of light. This indicates that **2** is noncytotoxic toward HT29 cells in darkness. However, upon illumination, the percentage of cells at the early apoptotic stage (i.e., externalization of phospholipid phosphatidylserine but not membrane leakage, annexin V-GFP$^+$/PI$^-$) increased from 2% to 92% when the concentration of **2** increased from 0 to 16 nM. The results for phthalocyanine **5** were similar and followed the same trend (data not shown). From these results, it can be concluded that these two photosensitizers induce apoptosis extensively.

The subcellular localization of these two conjugates in HT29 cells was also investigated by confocal microscopy. The cells were incubated with these conjugates together with LysoTracker Green DND 26 or MitoTracker Green FM, which are specific fluorescence dyes for lysosomes and mitochondria, respectively. As shown in Figure 7d, the fluorescence caused by the LysoTracker (excited at 488 nm, monitored at 500−570 nm) is well superimposed with the fluorescence caused by **2** (excited at 633 nm, monitored at 640−700 nm). The very similar fluorescence intensity profiles of **2** and LysoTracker traced along the green line in this figure (Figure 7e) also confirm that this compound can target lysosomes of the cells. By contrast, the fluorescence images of **2** and the MitoTracker (excited at 488 nm, monitored at 500−570 nm) cannot be superimposed (Figure 7i and Figure 7j), indicating that this compound is not localized in the mitochondria. The subcellular localization property of **5** in HT29 cells is similar to that of **2**. It can also target the lysosomes, but not the mitochondria, of the cells as shown in Figure S5 (Supporting Information).

In Vivo Studies. Phthalocyanines **2** and **5** were selected for in vivo evaluation of their PDT efficacy. Nude mice bearing a HT29 tumor were treated with an intravenous dose of the

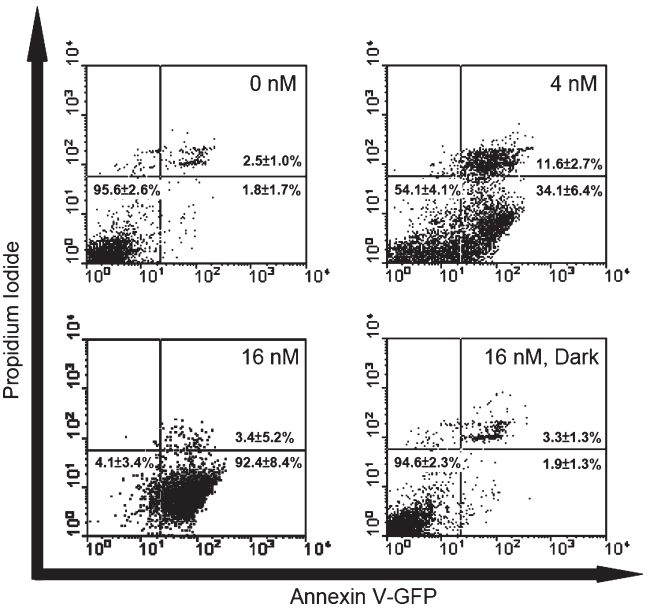

Figure 6. Flow cytometric analysis of the cell death mechanism induced by compound **2** upon PDT treatment ($\lambda > 610$ nm, 40 mW cm^{-2}, 48 J cm^{-2}) on HT29 cells. Data are expressed as mean values ± standard deviations of three independent experiments. The lower left quadrant of each panel shows the viable cells, negative for both annexin V-GFP and PI. The lower right quadrants represent the apoptotic cells (annexin V-GFP$^+$/PI$^-$), while the upper right quadrants represent the necrotic or late-stage apoptotic cells (annexin V-GFP$^+$/PI$^+$).

phthalocyanines (1 μmol kg^{-1}). The tumor was illuminated with a diode laser at 675 nm (total fluence of 30 J cm^{-2}) after 24 h of the injection. After the treatment, the tumor size was monitored continuously for 13 days. As shown in Figure 8, phthalocyanines **2** and **5** can effectively suppress the tumor growth in mice, while for all the controls including the light and drug-only conditions, the tumor continues to grow. The results suggest that both compounds also function as efficient photosensitizers in an animal model.

The in vivo toxicity of phthalocyanines **2** and **5** was also preliminary evaluated by using plasma enzyme activity assays. The blood of the mice was collected at the end of tumor regression study (13 days after PDT) by intracardiac puncture. The activity levels of the two hepatic enzymes aspartate aminotransferase (AST) and alanine aminotransferase (ALT) in the serum were measured. There were no significant differences in the activity levels for all the controls for both compounds (Figure S6 in the Supporting Information). The results indicated that these compounds did not cause apparent injury to the liver of the mice.

Conclusions

We have prepared and characterized a series of novel silicon(IV) phthalocyanines with polyamine moieties at the axial positions. These hydrophilic compounds are essentially nonaggregated in aqueous media, probably because of protonation of the amino groups, and exhibit a relatively high fluorescence quantum yield, which generally increases as the pH decreases. Upon illumination, these compounds are highly potent toward HT29 and CHO cells, particularly the former. Phthalocyanines **2** and **3** represent the most potent photosensitizers developed in our laboratory so far, which have IC_{50} values as low as ~1 nM against HT29 cells. As shown by confocal microscopy, compounds **2** and **5** exhibit high selectivity

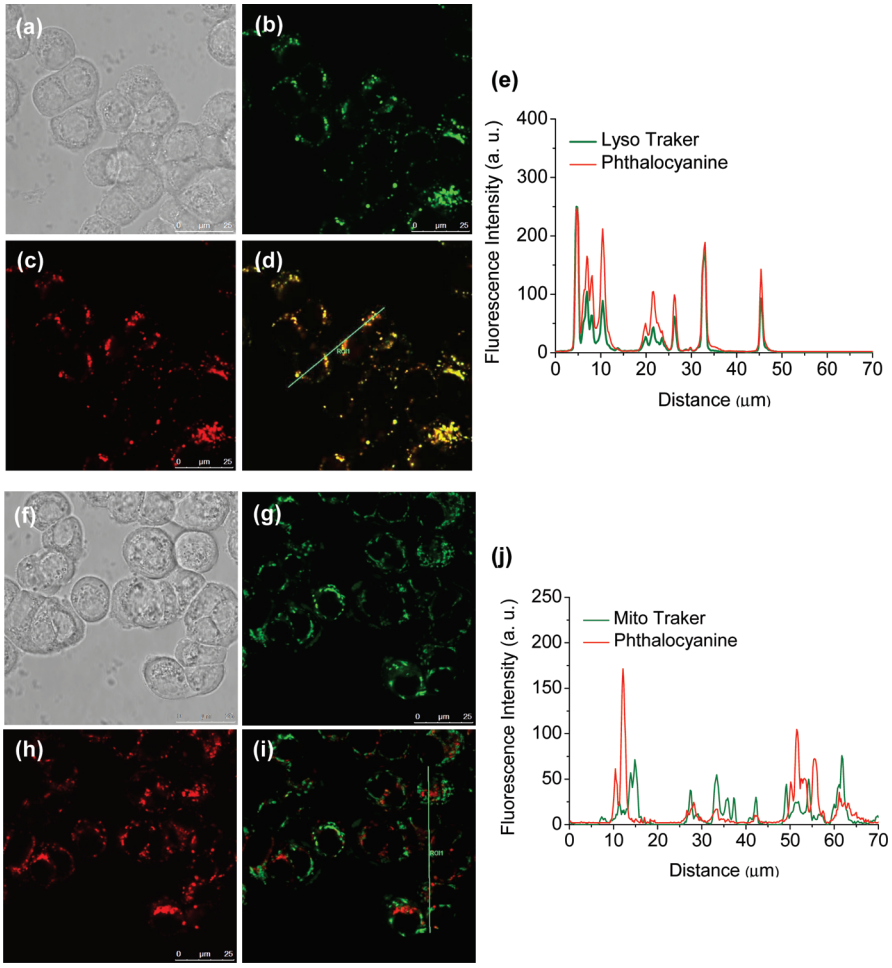

Figure 7. Visualization of the intracellular fluorescence of HT29 by using filter sets specific for (b) LysoTracker (in green) and (c) phthalocyanine **2** (in red). The corresponding superimposed image and the bright field image are given in (d) and (a), respectively. (e) shows the fluorescence intensity profiles of **2** (red) and LysoTracker (green) traced along the green line in (d). The corresponding images for **2** and the MitoTracker are shown in (f) to (j).

toward the lysosomes of HT29 cells inducing apoptosis extensively. These two compounds also effectively inhibit the growth of tumor in vivo. All these results show that these novel phthalocyanine−polyamine conjugates are highly promising photosensitizers for PDT. Further studies are deemed necessary to reveal the structure−activity relationships and the actual role of the polyamine moieties.

Experimental Section

Materials and Methods. All the reactions were performed under an atmosphere of nitrogen. THF and toluene were distilled from sodium benzophenone ketyl and sodium, respectively. DMF was dried over barium oxide and distilled under reduced pressure. Pyridine, CH_2Cl_2, and acetonitrile were distilled from calcium hydride. Chromatographic purifications were performed on silica gel (Macherey-Nagel, 230−400 mesh) columns with the indicated eluents. All other solvents and reagents were of reagent grade and used as received. Compounds **13**,[53] **20**,[54] and **30**[55] were prepared as described.

^1H and $^{13}C\{^1H\}$ NMR spectra were recorded on a Bruker DPX 300 spectrometer (^1H, 300 MHz; ^{13}C, 75.4 MHz) or Bruker Advance III 400 spectrometer (^1H, 400 MHz; ^{13}C, 100.6 MHz) in deuterated solvents. Spectra were referenced internally by using the residual solvent [^1H, $\delta = 3.31$ (for CD_3OD) or 7.26 (for $CDCl_3$)] or solvent [^{13}C, $\delta = 49.0$ (for CD_3OD) or 77.0 (for $CDCl_3$)] resonances relative to $SiMe_4$. Electron impact (EI), electrospray ionization (ESI), and fast-atom bombardment (FAB) mass spectra were recorded on a Thermo Finnigan MAT 95 XL mass spectrometer. The purity of all the phthalocyanines (**1**−**9**) was determined by elemental analysis performed by the Shanghai Institute of Organic Chemistry, Chinese Academy of Sciences, China, and was found to be ≥95%.

UV−vis and steady-state fluorescence spectra were taken on a Cary 5G UV−vis−NIR spectrophotometer and a Hitachi F-7000 spectrofluorometer, respectively. The Φ_F values were determined by the equation $\Phi_{F(sample)} = (F_{sample}/F_{ref})(A_{ref}/A_{sample})(n^2_{sample}/n^2_{ref})\Phi_{F(ref)}$,[56] where F, A, and n are the measured fluorescence (area under the emission peak), the absorbance at the excitation position (610 nm), and the refractive index of the solvent, respectively. ZnPc in DMF was used as the reference [$\Phi_{F(ref)} = 0.28$].[44] To minimize reabsorption of radiation by the ground-state species, the emission spectra were obtained in very dilute solutions of which the absorbance at 610 nm was about 0.03. The Φ_Δ values were measured in DMF by the method of chemical quenching of DPBF by using ZnPc as the reference ($\Phi_\Delta = 0.56$).[46]

Boc-Protected Hydroxyamine 14. A mixture of 3-amino-1-propanol (**10**) (10.0 g, 0.13 mol) and methanesulfonate **13** (5.1 g, 19.1 mmol) in acetonitrile (20 mL) was heated at 75 °C for 48 h. The solvent was then removed under reduced pressure. The residue was dissolved in CH_2Cl_2 (30 mL), and the solution was washed with 10% aqueous Na_2CO_3 solution (100 mL × 3). The organic portion was separated and dried over anhydrous Na_2SO_4. After evaporation in vacuo, the residue was purified by flash column chromatography using MeOH/$CHCl_3$ (1:9 v/v)

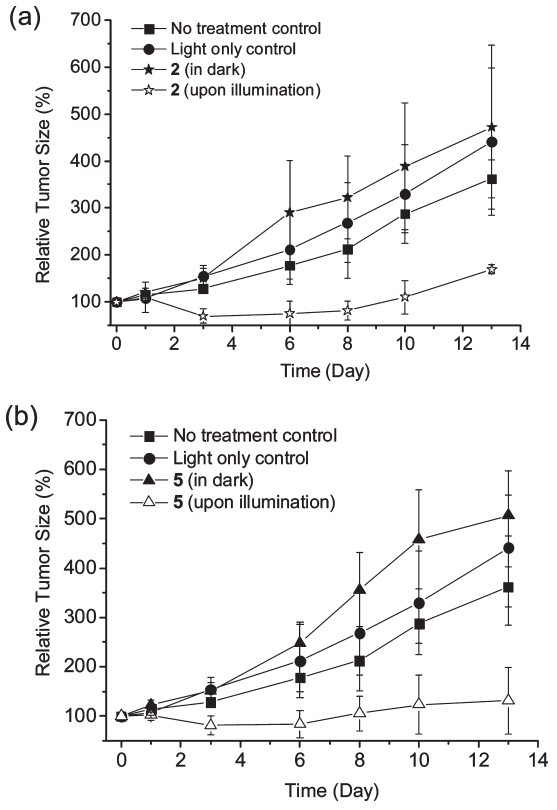

Figure 8. Tumor growth delay after PDT by phthalocyanines (a) **2** and (b) **5**. Nude mice bearing a HT29 tumor subcutaneously were treated with an intravenous dose of the drug (1 μmol kg^{-1}). Illumination with laser light (30 J cm^{-2}) was applied for the PDT (n = 5 for each group) and the light-only control (n = 3). The mice for drug-only control (n = 3 for each group) and no treatment control (n = 6) were kept in darkness. Data are expressed as mean values ± standard deviations.

as eluent to afford **14** as a pale yellow oil (1.6 g, 34%). ^{1}H NMR (300 MHz, $CDCl_3$): δ 3.81 (t, J = 5.1 Hz, 2 H, OCH_2), 3.28 (br s, 2 H, NCH_2), 2.83 (br s, 5 H, NCH_2 and NCH_3), 2.60 (t, J = 6.3 Hz, 2 H, NCH_2), 1.67−1.74 (m, 4 H, CH_2), 1.46 (s, 9 H, CH_3). MS (EI): m/z 246 (65%, M^+), 201 [100%, $(M - CH_2CH_2OH)^+$]. HRMS (EI): calcd for $C_{12}H_{26}N_2O_3$ (M^+) 246.1938, found 246.1935.

Boc-Protected Hydroxyamine 15. According to the procedure described for **14**, treatment of 2-(methylamino)ethanol (**11**) (3.8 g, 50.6 mmol) with methanesulfonate **13** (3.6 g, 13.5 mmol) in acetonitrile (20 mL) gave **15** as a yellow oil (2.0 g, 60%). ^{1}H NMR (400 MHz, $CDCl_3$): δ 3.59 (t, J = 5.2 Hz, 2 H, OCH_2), 3.26 (br s, 2 H, NCH_2), 2.85 (s, 3 H, NCH_3), 2.52 (t, J = 5.2 Hz, 2 H, NCH_2), 2.40 (t, J = 7.2 Hz, 2 H, NCH_2), 2.25 (s, 3 H, CH_3), 1.70 (quintet, J = 7.2 Hz, 2 H, CH_2), 1.46 (s, 9 H, CH_3). MS (EI): m/z 246 (1%, M^+), 215 [100%, $(M - CH_2OH)^+$]. HRMS (EI): calcd for $C_{12}H_{26}N_2O_3$ (M^+) 246.1938, found 246.1935.

Boc-Protected Hydroxyamine 16. According to the procedure described for **14**, treatment of 3-(methylamino)-1-propanol (**12**) (10.0 g, 0.11 mol) with methanesulfonate **13** (4.9 g, 18.3 mmol) in acetonitrile (20 mL) gave **16** as a yellow oil (1.6 g, 33%). ^{1}H NMR (300 MHz, $CDCl_3$): δ 3.80 (t, J = 5.1 Hz, 2 H, OCH_2), 3.23 (virtual t, 2 H, NCH_2), 2.85 (s, 3 H, NCH_3), 2.59 (t, J = 5.7 Hz, 2 H, NCH_2), 2.34 (t, J = 7.5 Hz, 2 H, NCH_2), 2.25 (s, 3 H, NCH_3), 1.64−1.78 (m, 4 H, CH_2), 1.46 (s, 9 H, CH_3). MS (EI): m/z 260 (23%, M^+), 215 [32%, $(M - CH_2CH_2OH)^+$]. HRMS (EI): calcd for $C_{13}H_{28}N_2O_3$ (M^+) 260.2094, found 260.2096.

Hydroxyamine 17. A solution of Boc-protected hydroxyamine **14** (1.5 g, 6.1 mmol) in MeOH (10 mL) was cooled in an ice bath for 10 min. A solution of HCl (4 M, 10 mL) was added dropwise. Then the mixture was stirred at 0 °C for 20 min and then at room temperature for 16 h. The solvent was removed under reduce pressure. The yellow solid residue was neutralized by aqueous Na_2CO_3 solution (20% w/w, 10 mL). The solvent was removed, and the residue was dissolved in CH_2Cl_2 (50 mL). After filtration, the filtrate was dried with anhydrous Na_2SO_4 and evaporated in vacuo to give the product as a colorless oil (0.82 g, 92%). ^{1}H NMR (400 MHz, $CDCl_3$): δ 3.78 (t, J = 5.6 Hz, 2 H, OCH_2), 2.85 (t, J = 5.6 Hz, 2 H, NCH_2), 2.67 (t, J = 6.8 Hz, 2 H, NCH_2), 2.62 (t, J = 6.8 Hz, 2 H, NCH_2), 2.42 (s, 3 H, NCH_3), 1.65−1.71 (m, 4 H, CH_2). ^{13}C{^{1}H} NMR (75.4 MHz, $CDCl_3$): δ 64.1, 50.2, 49.9, 48.1, 36.5, 30.7, 29.9. MS (EI): m/z 146 (9%, M^+), 115 [100%, $(M - CH_2OH)^+$]. HRMS (EI): calcd for $C_7H_{18}N_2O$ (M^+) 146.1414, found 146.1411.

Hydroxyamine 18. According to the procedure described for **17**, treatment of Boc-protected hydroxyamine **15** (1.8 g, 7.3 mmol) in MeOH (10 mL) with HCl (4 M, 10 mL) followed by neutralization with aqueous Na_2CO_3 solution (20% w/w, 10 mL) gave **18** as a colorless oil (0.99 g, 93%). ^{1}H NMR (400 MHz, $CDCl_3$): δ 3.61 (t, J = 5.2 Hz, 2 H, OCH_2), 2.69 (t, J = 6.8 Hz, 2 H, NCH_2), 2.48−2.54 (m, 4 H, NCH_2), 2.44 (s, 3 H, NCH_3), 2.26 (s, 3 H, NCH_3), 1.69 (quintet, J = 6.8 Hz, 2 H, CH_2). ^{13}C{^{1}H} NMR (100.6 MHz, $CDCl_3$): δ 58.8 (two overlapping signals), 55.1, 50.2, 42.2, 36.1, 26.7. MS (ESI): m/z 147 [100%, $(M + H)^+$]. HRMS (ESI): calcd for $C_7H_{19}N_2O$ $(M + H)^+$ 147.1492, found 147.1490.

Hydroxyamine 19. According to the procedure described for **17**, treatment of Boc-protected hydroxyamine **16** (1.6 g, 6.1 mmol) in MeOH (10 mL) with HCl (4 M, 10 mL) followed by neutralization with aqueous Na_2CO_3 solution (20% w/w, 10 mL) afforded **19** as a colorless oil (0.83 g, 85%). ^{1}H NMR (300 MHz, $CDCl_3$): δ 3.79 (t, J = 5.1 Hz, 2 H, OCH_2), 2.57−2.63 (m, 4 H, NCH_2), 2.41−2.46 (m, 5 H, NCH_2 and NCH_3), 2.25 (s, 3 H, NCH_3), 1.66−1.73 (m, 4 H, CH_2). ^{13}C{^{1}H} NMR (75.4 MHz, $CDCl_3$): δ 64.2, 58.0, 56.1, 50.1, 41.9, 36.5, 27.8, 27.4. MS (EI): m/z 160 (76%, M^+), 129 [100%, $(M - CH_2OH)^+$]. HRMS (EI): calcd for $C_8H_{20}N_2O$ (M^+) 160.1570, found 160.1576.

Methanesulfonate 21. A solution of Boc-protected hydroxyamine **20** (5.0 g, 24.6 mmol) and triethylamine (25 mL) in CH_2Cl_2 (130 mL) was stirred at 0 °C by using an ice bath. Methanesulfonyl chloride (5.8 g, 50.6 mmol) was added slowly over 30 min under a nitrogen atmosphere. The reaction mixture was stirred at 0 °C for 1 h. Then it was stirred at room temperature for 16 h. The mixture was cooled to 0 °C, and then NaOH solution (4 M, 50 mL) was added slowly with vigorous stirring. The organic portion was separated and washed with water (70 mL × 3). It was then dried over anhydrous Na_2SO_4 and evaporated in vacuo to give the product as a yellow oil (6.3 g, 91%). The product was used in the next step without further purification. ^{1}H NMR (400 MHz, $CDCl_3$): δ 4.26 (t, J = 6.4 Hz, 2 H, OCH_2), 3.26 (t, J = 6.4 Hz, 2 H, NCH_2), 3.02 (s, 3 H, SCH_3), 2.84 (s, 3 H, NCH_3), 1.70−1.78 (m, 2 H, CH_2), 1.60−1.68 (m, 2 H, CH_2), 1.46 (s, 9 H, CH_3).

Boc-Protected Hydroxyamine 22. According to the procedure described for **14**, treatment of 3-amino-1-propanol (**10**) (10.0 g, 0.13 mol) with methanesulfonate **21** (5.1 g, 18.1 mmol) in acetonitrile (20 mL) gave **22** as a yellow oil (1.7 g, 36%). ^{1}H NMR (400 MHz, $CDCl_3$): δ 3.81 (t, J = 5.2 Hz, 2 H, OCH_2), 3.21 (br s, 2 H, NCH_2), 2.88 (t, J = 5.2 Hz, 2 H, NCH_2), 2.83 (s, 3 H, NCH_3), 2.63 (t, J = 6.8 Hz, 2 H, NCH_2), 1.69 (quintet, J = 5.2 Hz, 2 H, CH_2), 1.50−1.54 (m, 2 H, CH_2), 1.43−1.49 (m, 11 H, CH_2 and CH_3). MS (EI): m/z 260 (50%, M^+), 215 [100%, $(M - CH_2CH_2OH)^+$]. HRMS (EI): calcd for $C_{13}H_{28}N_2O_3$ (M^+) 260.2094, found 260.2093.

Boc-Protected Hydroxyamine 23. According to the procedure described for **14**, treatment of 3-methylamino-1-propanol (**12**) (10.1 g, 0.11 mol) with methanesulfonate **21** (5.0 g, 17.8 mmol) in acetonitrile (20 mL) gave **23** as a yellow oil (2.4 g, 49%). ^{1}H NMR (400 MHz, $CDCl_3$): δ 3.80 (t, J = 5.2 Hz, 2 H, OCH_2), 3.22 (br s, 2 H, NCH_2), 2.83 (s, 3 H, NCH_3), 2.59 (t, J = 5.2 Hz, 2 H, NCH_2), 2.38 (t, J = 7.2 Hz, 2 H, NCH_2), 2.24 (s, 3 H, NCH_3),

1.70 (quintet, J = 5.2 Hz, 2 H, CH_2), 1.48−1.51 (m, 4 H, CH_2), 1.45 (s, 9 H, CH_3). MS (EI): m/z 274 (25%, M^+), 229 [70%, $(M - CH_2CH_2OH)^+$]. HRMS (EI): calcd for $C_{14}H_{30}N_2O_3$ (M^+) 274.2251, found 274.2242.

Hydroxyamine 24. According to the procedure described for **17**, treatment of Boc-protected hydroxylamine **22** (1.5 g, 5.8 mmol) in MeOH (10 mL) with HCl (4 M, 10 mL) followed by neutralization with aqueous Na_2CO_3 solution (20% w/w, 10 mL) gave **24** as a colorless oil (0.85 g, 91%). ^{1}H NMR (400 MHz, $CDCl_3$): δ 3.80 (t, J = 5.6 Hz, 2 H, OCH_2), 2.87 (t, J = 5.6 Hz, 2 H, NCH_2), 2.63 (virtual t, J = 6.4 Hz, 2 H, NCH_2), 2.57 (virtual t, J = 6.4 Hz, 2 H, NCH_2), 2.42 (s, 3 H, NCH_3), 1.69 (quintet, J = 5.6 Hz, 2 H, CH_2), 1.50−1.53 (m, 4 H, CH_2). ^{13}C{^{1}H} NMR (75.4 MHz, $CDCl_3$): δ 64.6, 51.9, 50.1, 49.7, 36.5, 30.5, 27.7, 27.6. MS (EI): m/z 160 (40%, M^+), 115 [100%, $(M - CH_2CH_2OH)^+$]. HRMS (EI): calcd for $C_8H_{20}N_2O$ (M^+) 160.1570, found 160.1567.

Hydroxyamine 25. According to the procedure described for **17**, treatment of Boc-protected hydroxylamine **23** (1.5 g, 5.5 mmol) in MeOH (10 mL) with HCl (4 M, 10 mL) followed by neutralization with aqueous Na_2CO_3 solution (20% w/w, 10 mL) gave **25** as a colorless oil (0.66 g, 69%). ^{1}H NMR (400 MHz, $CDCl_3$): δ 3.80 (t, J = 5.2 Hz, 2 H, OCH_2), 2.57−2.61 (m, 4 H, NCH_2), 2.43 (s, 3 H, NCH_3), 2.38 (t, J = 6.8 Hz, 2 H, NCH_2), 2.24 (s, 3 H, NCH_3), 1.67−1.72 (m, 2 H, CH_2), 1.45−1.54 (m, 4 H, CH_2). ^{13}C{^{1}H} NMR (100.6 MHz, $CDCl_3$): δ 64.7, 58.5, 58.1, 51.9, 41.9, 36.4, 27.6 (two overlapping signals), 25.0. MS (EI): m/z 174 (25%, M^+), 102 [100%, $(HO(CH_2)_3N(CH_3)CH_2)^+$]. HRMS (EI): calcd for $C_9H_{22}N_2O$ (M^+) 174.1727, found 174.1723.

Boc-Protected Hydroxyamine 26. A solution of **14** (5.1 g, 20.7 mmol) in triethylamine/MeOH (1:7 v/v, 150 mL) was stirred at 0 °C for 10 min. Di-*tert*-butyl dicarbonate (10.5 g, 48.1 mmol) in MeOH (50 mL) was added slowly over 10 min under a nitrogen atmosphere. The mixture was stirred at 0 °C for 1 h and then at room temperature for 16 h. The solvent was removed under reduced pressure. The oily residue was dissolved in CH_2Cl_2 (100 mL), and the resulting solution was washed with water (100 mL × 3). The organic layer was separated, dried over anhydrous Na_2SO_4, and evaporated to give **26** as a colorless oil (6.5 g, 91%). ^{1}H NMR (300 MHz, $CDCl_3$): δ 3.54 (br s, 2 H, OCH_2), 3.38 (br s, 2 H, NCH_2), 3.09−3.20 (m, 4 H, NCH_2), 2.85 (s, 3 H, NCH_3), 1.59−1.82 (m, 4 H, CH_2), 1.47 (s, 9 H, CH_3), 1.46 (s, 9 H, CH_3). MS (EI): m/z 346 (38%, M^+). HRMS (EI): calcd for $C_{17}H_{34}N_2O_5$ (M^+) 346.2462, found 346.2460.

Methanesulfonate 27. According to the procedure described for **21**, treatment of Boc-protected hydroxylamine **26** (5.1 g, 14.7 mmol) with methanesulfonyl chloride (10.1 g, 88.2 mmol) in the presence of triethylamine (25 mL) in CH_2Cl_2 (130 mL) gave **27** as a yellow oil (5.2 g, 83%). ^{1}H NMR (300 MHz, $CDCl_3$): δ 4.25 (t, J = 6.3 Hz, 2 H, OCH_2), 3.26−3.37 (m, 2 H, NCH_2), 3.11−3.24 (m, 4 H, NCH_2), 3.03 (s, 3 H, SCH_3), 2.85 (s, 3 H, NCH_3), 1.92−2.04 (m, 2 H, CH_2), 1.70−1.79 (m, 2 H, CH_2), 1.46 (s, 18 H, CH_3).

Boc-Protected Hydroxyamine 28. According to the procedure described for **14**, treatment of **27** (5.1 g, 12.0 mmol) with 3-(methylamino)-1-propanol (**12**) (5.1 g, 57.2 mmol) in acetonitrile (20 mL) gave **28** as a colorless oil (3.0 g, 60%). ^{1}H NMR (400 MHz, $CDCl_3$): δ 3.79 (t, J = 5.6 Hz, 2 H, OCH_2), 3.20 (br s, 6 H, NCH_2), 2.85 (s, 3 H, NCH_3), 2.59 (t, J = 5.6 Hz, 2 H, NCH_2), 2.37 (t, J = 7.2 Hz, 2 H, NCH_2), 2.25 (s, 3 H, NCH_3), 1.68−1.75 (m, 6 H, CH_2), 1.46 (s, 18 H, CH_3). MS (EI): m/z 417 (12%, M^+), 372 [17%, $(M - CH_2CH_2OH)^+$], 102 [100%, $(HO(CH_2)_3N(CH_3)CH_2)^+$]. HRMS (EI): calcd for $C_{21}H_{43}N_3O_5$ (M^+) 417.3197, found 417.3187.

Hydroxyamine 29. According to the procedure described for **17**, treatment of Boc-protected hydroxylamine **28** (1.6 g, 3.8 mmol) in MeOH (10 mL) with HCl (4 M, 10 mL) followed by neutralization with aqueous Na_2CO_3 solution (20% w/w, 10 mL) gave **29** as a colorless oil (0.69 g, 84%). ^{1}H NMR (400 MHz, $CDCl_3$): δ 3.78 (t, J = 5.6 Hz, 2 H, OCH_2), 2.61−2.68 (m, 6 H, NCH_2), 2.58 (t, J = 5.6 Hz, 2 H, NCH_2), 2.40−2.44 (m, 5 H, NCH_2 and NCH_3), 2.24 (s, 3 H, NCH_3), 1.65−1.72 (m, 6 H, CH_2). ^{13}C{^{1}H} NMR (100.6 MHz, $CDCl_3$): δ 64.2, 58.0, 56.2, 50.5, 48.4, 48.1, 42.0, 36.5, 30.0, 27.8, 27.6. MS (EI): m/z 217 (25%, M^+), 102 [100%, $(HO(CH_2)_3N(CH_3)CH_2)^+$]. HRMS (EI): calcd for $C_{11}H_{27}N_3O$ (M^+) 217.2149, found 217.2153.

Phthalocyanine 1. A mixture of silicon(IV) phthalocyanine dichloride (0.20 g, 0.33 mmol), 2-(methylamino)ethanol (**11**) (0.22 g, 2.93 mmol), and pyridine (0.5 mL) in toluene (30 mL) was refluxed for 4 h. After evaporation of the solvent in vacuo, the residue was dissolved in CH_2Cl_2 (100 mL) and then washed with water (100 mL × 3). The organic layer was collected and evaporated under reduced pressure. The crude product was recrystallized from $CHCl_3$/1-hexane (1:4 v/v) to give the product as a blue solid (0.18 g, 79%). ^{1}H NMR (400 MHz, $CDCl_3$): δ 9.63−9.65 (m, 8 H, Pc-H_α), 8.34−8.36 (m, 8 H, Pc-H_β), 0.73 (s, 6 H, NCH_3), −0.38 (t, J = 5.2 Hz, 4 H, CH_2), −2.00 (t, J = 5.2 Hz, 4 H, OCH_2). ^{13}C{^{1}H} NMR (100.6 MHz, $CDCl_3$): δ 149.2, 135.9, 131.0, 123.7, 53.5, 50.1, 34.0. MS (FAB): m/z 688 (7%, M^+), 614 [100%, $(M - OCH_2CH_2NHCH_3)^+$]. HRMS (FAB): calcd for $C_{38}H_{32}N_{10}O_2Si$ (M^+) 688.2473, found 688.2459. Anal. Calcd for $C_{38}H_{32}N_{10}O_2Si$: C, 66.26; H, 4.68; N, 20.33. Found: C, 65.72; H, 4.55; N, 19.89.

Phthalocyanine 2. According to the procedure described for **1**, silicon(IV) phthalocyanine dichloride (0.15 g, 0.25 mmol) was treated with 3-(methylamino)-1-propanol (**12**) (0.21 g, 2.36 mmol) and pyridine (0.5 mL) in toluene (30 mL) to give **2** as a blue solid (0.13 g, 72%). ^{1}H NMR (400 MHz, $CDCl_3$): δ 9.63−9.65 (m, 8 H, Pc-H_α), 8.33−8.35 (m, 8 H, Pc-H_β), 1.16 (s, 6 H, NCH_3), −0.08 (t, J = 6.4 Hz, 4 H, NCH_2), −1.33 (virtual quintet, J = 6.0 Hz, 4 H, CH_2), −2.04 (t, J = 5.6 Hz, 4 H, OCH_2). ^{13}C{^{1}H} NMR (100.6 MHz, $CDCl_3$): δ 149.2, 135.9, 130.9, 123.6, 53.9, 47.9, 35.2, 28.6. MS (FAB): m/z 717 [3%, $(M + H)^+$], 628 [55%, $(M - O(CH_2)_3NHCH_3)^+$]. HRMS (FAB): calcd for $C_{40}H_{37}N_{10}O_2Si$ $(M + H)^+$ 717.2865, found 717.2863. Anal. Calcd for $C_{40}H_{36}N_{10}O_2Si$: C, 67.02; H, 5.06; N, 19.54. Found: C, 66.92; H, 5.23; N, 19.32.

Phthalocyanine 3. According to the procedure described for **1**, silicon(IV) phthalocyanine dichloride (0.15 g, 0.25 mmol) was treated with 4-(methylamino)-1-butanol (**30**) (0.25 g, 2.43 mmol) and pyridine (0.5 mL) in toluene (30 mL) to give **3** as a blue solid (0.14 g, 76%). ^{1}H NMR (400 MHz, $CDCl_3$): δ 9.62−9.64 (m, 8 H, Pc-H_α), 8.32−8.34 (m, 8 H, Pc-H_β), 1.61 (s, 6 H, NCH_3), 0.76 (t, J = 7.2 Hz, 4 H, NCH_2), −1.18 (quintet, J = 7.2 Hz, 4 H, CH_2), −1.62 (virtual quintet, J = 6.8 Hz, 4 H, CH_2), −2.09 (t, J = 6.0 Hz, 4 H, OCH_2). ^{13}C{^{1}H} NMR (100.6 MHz, $CDCl_3$): δ 149.2, 136.0, 130.8, 123.7, 54.6, 50.1, 35.5, 26.7, 24.1. MS (FAB): m/z 745 [10%, $(M + H)^+$], 642 [100%, $(M - O(CH_2)_4NHCH_3)^+$]. HRMS (FAB): calcd for $C_{42}H_{41}N_{10}O_2Si$ $(M + H)^+$ 745.3178, found 745.3195. Anal. Calcd for $C_{42}H_{42}N_{10}O_3Si$ (**3**·H_2O): C, 66.12; H, 5.55; N, 18.36. Found: C, 66.72; H, 5.58; N, 17.88.

Phthalocyanine 4. According to the procedure described for **1**, silicon(IV) phthalocyanine dichloride (0.13 g, 0.21 mmol) was treated with hydroxyamine **17** (0.23 g, 1.57 mmol) and pyridine (0.5 mL) in toluene (30 mL) to give **4** as a blue solid (0.11 g, 63%). ^{1}H NMR (300 MHz, $CDCl_3$): δ 9.63−9.66 (m, 8 H, Pc-H_α), 8.34−8.37 (m, 8 H, Pc-H_β), 2.25 (s, 6 H, NCH_3), 2.05 (t, J = 7.2 Hz, 4 H, NCH_2), 1.29 (t, J = 7.2 Hz, 4 H, NCH_2), 0.73 (quintet, J = 7.2 Hz, 4 H, CH_2), −0.06 (t, J = 6.3 Hz, 4 H, NCH_2), −1.35 (virtual quintet, J = 6.0 Hz, 4 H, CH_2), −2.06 (t, J = 5.7 Hz, 4 H, OCH_2). ^{13}C{^{1}H} NMR (75.4 MHz, $CDCl_3$): δ 149.2, 135.9, 130.9, 123.7, 53.8, 50.0, 47.0, 45.6, 36.3, 29.3, 28.7. MS (FAB): m/z 831 [9%, $(M + H)^+$], 685 [47%, $(M - O(CH_2)_3NH(CH_2)_3NHCH_3)^+$]. HRMS (FAB): calcd for $C_{46}H_{51}N_{12}O_2Si$ $(M + H)^+$ 831.4022, found 831.4040. Anal. Calcd for $C_{46}H_{52}N_{12}O_3Si$ (**4**·H_2O): C, 65.07; H, 6.17; N, 19.80. Found: C, 65.50; H, 5.98; N, 19.50.

Phthalocyanine 5. According to the procedure described for **1**, silicon(IV) phthalocyanine dichloride (0.14 g, 0.23 mmol) was treated with hydroxyamine **24** (0.28 g, 1.75 mmol) and pyridine (0.5 mL) in toluene (30 mL) to give **5** as a blue solid (0.12 g, 61%). ^{1}H NMR (400 MHz, CD_3OD): δ 9.69−9.72 (m, 8 H, Pc-H_α), 8.46−8.48 (m, 8 H, Pc-H_β), 2.29 (s, 6 H, NCH_3), 2.26 (t, J = 7.6 Hz, 4 H, NCH_2), 1.24 (t, J = 7.6 Hz, 4 H, NCH_2), 1.01 (quintet, J = 7.6 Hz, 4 H, CH_2), 0.58 (quintet, J = 7.6 Hz, 4 H, CH_2), −0.11 (t, J = 6.8 Hz, 4 H, NCH_2), −1.26 to −1.20 (m, 4 H, CH_2), −1.99 (t, J = 5.6 Hz, 4 H, OCH_2). ^{13}C{^{1}H} NMR (100.6 MHz, $CDCl_3$): δ 149.2, 135.9, 130.9, 123.6, 53.8, 51.7, 48.7, 45.5, 36.3, 28.6, 27.2, 27.0. MS (FAB): m/z 859 [25%, $(M + H)^+$], 699 [100%, $(M - O(CH_2)_3NH(CH_2)_4NHCH_3)^+$]. HRMS (FAB): calcd for $C_{48}H_{55}N_{12}O_2Si$ $(M + H)^+$ 859.4335, found 859.4347. Anal. Calcd for $C_{48}H_{56}N_{12}O_3Si$ (**5**·H_2O): C, 65.73; H, 6.44; N, 19.16. Found: C, 65.90; H, 6.26; N, 18.63.

Phthalocyanine 6. According to the procedure described for **1**, silicon(IV) phthalocyanine dichloride (0.15 g, 0.25 mmol) was treated with hydroxyamine **18** (0.25 g, 1.71 mmol) and pyridine (0.5 mL) in toluene (30 mL) to give **6** as a blue solid (0.13 g, 63%). ^{1}H NMR (300 MHz, $CDCl_3$): δ 9.61−9.65 (m, 8 H, Pc-H_α), 8.32−8.35 (m, 8 H, Pc-H_β), 2.06 (s, 6 H, NCH_3), 1.63 (t, J = 7.2 Hz, 4 H, NCH_2), 0.44−0.49 (m, 10 H, NCH_2 and NCH_3), 0.32 (virtual quintet, J = 7.5 Hz, 4 H, CH_2), −0.79 (t, J = 6.3 Hz, 4 H, NCH_2), −1.97 (t, J = 6.3 Hz, 4 H, OCH_2). ^{13}C{^{1}H} NMR (75.4 MHz, $CDCl_3$): δ 149.2, 136.0, 130.8, 123.6, 56.0, 54.3, 53.3, 49.7, 41.1, 36.2, 26.5. MS (FAB): m/z 831 [8%, $(M + H)^+$], 685 [92%, $(M - OCH_2CH_2N(CH_3)(CH_2)_3NHCH_3)^+$]. HRMS (FAB): calcd for $C_{46}H_{51}N_{12}O_2Si$ $(M + H)^+$ 831.4022, found 831.4025. Anal. Calcd for $C_{46}H_{52}N_{12}O_3Si$ (**6**·H_2O): C, 65.07; H, 6.17; N, 19.80. Found: C, 64.99; H, 6.13; N, 19.24.

Phthalocyanine 7. According to the procedure described for **1**, silicon(IV) phthalocyanine dichloride (0.20 g, 0.33 mmol) was treated with hydroxyamine **19** (0.20 g, 1.25 mmol) and pyridine (0.5 mL) in toluene (30 mL) to give **7** as a blue solid (0.18 g, 64%). ^{1}H NMR (400 MHz, $CDCl_3$): δ 9.62−9.64 (m, 8 H, Pc-H_α), 8.32−8.35 (m, 8 H, Pc-H_β), 2.18 (s, 6 H, NCH_3), 1.99 (t, J = 7.2 Hz, 4 H, NCH_2), 1.15 (t, J = 7.2 Hz, 4 H, NCH_2), 1.03 (s, 6 H, NCH_3), 0.72 (quintet, J = 7.2 Hz, 4 H, CH_2), −0.57 (t, J = 7.6 Hz, 4 H, NCH_2), −1.52 to −1.45 (m, 4 H, CH_2), −2.06 (t, J = 6.0 Hz, 4 H, OCH_2). ^{13}C{^{1}H} NMR (100.6 MHz, $CDCl_3$): δ 149.2, 136.0, 130.8, 123.6, 54.6, 53.2, 52.3, 50.1, 41.3, 36.3, 26.5 (two overlapping signals). MS (FAB): m/z 859 [17%, $(M + H)^+$], 699 [100%, $(M - O(CH_2)_3N(CH_3)(CH_2)_3NHCH_3)^+$]. HRMS (FAB): calcd for $C_{48}H_{55}N_{12}O_2Si$ $(M + H)^+$ 859.4335, found 859.4350. Anal. Calcd for $C_{48}H_{56}N_{12}O_3Si$ (**7**·H_2O): C, 65.73; H, 6.44; N, 19.16. Found: C, 66.20; H, 6.29; N, 18.85.

Phthalocyanine 8. According to the procedure described for **1**, silicon(IV) phthalocyanine dichloride (0.25 g, 0.41 mmol) was treated with hydroxyamine **25** (0.41 g, 2.35 mmol) and pyridine (0.5 mL) in toluene (30 mL) to give **8** as a blue solid (0.19 g, 52%). ^{1}H NMR (400 MHz, CD_3OD): δ 9.66−9.68 (m, 8 H, Pc-H_α), 8.43−8.46 (m, 8 H, Pc-H_β), 2.28 (s, 6 H, NCH_3), 2.22 (t, J = 7.6 Hz, 4 H, NCH_2), 1.20 (t, J = 7.6 Hz, 4 H, NCH_2), 1.04 (s, 6 H, NCH_3), 1.00 (quintet, J = 7.6 Hz, 4 H, CH_2), 0.56 (quintet, J = 7.6 Hz, 4 H, CH_2), −0.66 (t, J = 7.6 Hz, 4 H, NCH_2), −1.38 to −1.31 (m, 4 H, CH_2), −2.00 (t, J = 5.6 Hz, 4 H, OCH_2). ^{13}C{^{1}H} NMR (100.6 MHz, CD_3OD): δ 150.8, 137.1, 132.8, 124.8, 57.4, 54.5, 53.0, 52.2, 41.2, 35.9, 27.8, 26.9, 24.5. MS (FAB): m/z 887 [7%, $(M + H)^+$], 713 [100%, $(M - O(CH_2)_3N(CH_3)(CH_2)_4NHCH_3)^+$]. HRMS (FAB): calcd for $C_{50}H_{59}N_{12}O_2Si$ $(M + H)^+$ 887.4648, found 887.4682. Anal. Calcd for $C_{50}H_{60}N_{12}O_3Si$ (**8**·H_2O): C, 66.35; H, 6.68; N, 18.57. Found: C, 66.90; H, 6.27; N, 18.14.

Phthalocyanine 9. According to the procedure described for **1**, silicon(IV) phthalocyanine dichloride (0.19 g, 0.31 mmol) was treated with hydroxyamine **29** (0.34 g, 1.56 mmol) and pyridine (0.5 mL) in toluene (30 mL) to give **9** as a blue solid (0.14 g, 46%). ^{1}H NMR (400 MHz, CD_3OD): δ 9.67−9.69 (m, 8 H, Pc-H_α), 8.44−8.46 (m, 8 H, Pc-H_β), 2.46 (t, J = 7.2 Hz, 4 H, NCH_2), 2.30−2.35 (m, 10 H, NCH_2 and NCH_3), 2.02 (t, J = 7.2 Hz, 4 H, NCH_2), 1.50 (quintet, J = 7.2 Hz, 4 H, CH_2), 1.21 (t, J = 7.2 Hz, 4 H, NCH_2), 1.06 (s, 6 H, NCH_3), 0.78 (quintet, J = 7.2 Hz, 4 H, CH_2), −0.59 (t, J = 7.6 Hz, 4 H, NCH_2), −1.39 to −1.33 (m, 4 H, CH_2), −1.98 (t, J = 5.6 Hz, 4 H, OCH_2). ^{13}C{^{1}H} NMR (100.6 MHz, CD_3OD): δ 150.8, 137.1, 132.8, 124.8, 55.4, 54.5, 53.4, 50.5, 48.4, 48.3, 41.3, 35.8, 29.3, 27.1, 26.2. MS (FAB): m/z 973 [4%, $(M + H)^+$], 756 [35%, $(M - O(CH_2)_3N(CH_3)(CH_2)_3NH(CH_2)_3NHCH_3)^+$]. HRMS (FAB): calcd for $C_{54}H_{69}N_{14}O_2Si$ $(M + H)^+$ 973.5492, found 973.5466. Anal. Calcd for $C_{54}H_{72}N_{14}O_4Si$ (**9**·$2H_2O$): C, 64.26; H, 7.19; N, 19.43. Found: C, 64.40; H, 6.69; N, 19.19.

Cell Lines and Culture Conditions. The HT29 human colorectal carcinoma cells (from ATCC, no. HTB-38) were maintained in Dulbecco's modified Eagle's medium (DMEM; Invitrogen, no. 10313-021) supplemented with fetal calf serum (10%), penicillin−streptomycin (100 units mL^{-1} and 100 μg mL^{-1}, respectively), L-glutamine (2 mM), aminoguanidine (2 mM), and transferrin (10 μg mL^{-1}). The CHO cells (from ATCC, no. CCL-61) were maintained in RPMI medium 1640 (Invitrogen, no. 23400-021) supplemented with fetal calf serum (10%), aminoguanidine (2 mM), and penicillin−streptomycin (100 units mL^{-1} and 100 μg mL^{-1}, respectively). Approximately 3×10^4 cells per well in the media were inoculated in 96-multiwell plates and incubated overnight at 37 °C in a humidified 5% CO_2 atmosphere.

Photocytotoxicity Assay. Phthalocyanines **1**−**3** and **4**−**9** were first dissolved in THF and MeOH to give 1.6 and 1.0 mM solutions, respectively, which were diluted to appropriate concentrations with the culture medium. The cells, after being rinsed with phosphate buffered saline (PBS), were incubated with 100 μL of these phthalocyanine solutions for 2 h at 37 °C under 5% CO_2. The cells were then rinsed again with PBS and refilled with 100 μL of the culture medium before being illuminated at ambient temperature. The light source consisted of a 300 W halogen lamp, a water tank for cooling, and a color glass filter (Newport) (cut-on 610 nm). The fluence rate (λ > 610 nm) was 40 mW cm^{-2}. Illumination of 20 min led to a total fluence of 48 J cm^{-2}. Alternatively, the cells were illuminated with a diode laser (Biolitec Ceralas) at 675 nm operated at 0.2 W. Illumination on a spot size of 1.13 cm^2 for 11.3, 22.6, 33.9, 45.2, 67.8, and 90.4 s led to a total fluence of 2, 4, 6, 8, 12, and 16 J cm^{-2}, respectively.

Cell viability was determined by means of the colorimetric MTT assay.[57] After illumination, the cells were incubated at 37 °C under 5% CO_2 overnight. An MTT (Sigma) solution in PBS (3 mg mL^{-1}, 50 μL) was added to each well followed by incubation for 2 h under the same environment. A solution of sodium dodecyl sulfate (Sigma, 10% by weight, 50 μL) was then added to each well. The plate was incubated in an oven at 60 °C for 30 min. Then 80 μL of isopropanol was added to each well. The plate was agitated on a Bio-Rad microplate reader at ambient temperature for 10 s before the absorbance at 540 nm for each well was taken. The average absorbance of the blank wells, which did not contain the cells, was subtracted from the readings of the other wells. The cell viability was then determined by the following equation: % viability = $[\sum(A_i/A_{control} \times 100)]/n$, where A_i is the absorbance of the ith data (i = 1, 2, ..., n), $A_{control}$ is the average absorbance of the control wells in which the phthalocyanine was absent, and n (=4) is the number of the data points.

Subcellular Localization Studies. About 3×10^4 HT29 cells in the culture medium (2 mL) were seeded on a coverslip and incubated overnight at 37 °C under 5% CO_2. The medium was then removed. The cells were incubated with a solution of **2** or **5** in the medium (1 μM, 2 mL) for 2 h under the same conditions. For the study using LysoTracker, the cells were incubated with LysoTracker Green DND 26 (Molecular Probes, 4 μM in the culture medium) under these conditions for a further 15 min. For the study using MitoTracker, the cells were incubated with

MitoTracker Green FM (Molecular Probes, 0.2 μM) in the medium (2 mL) for a further 30 min. For both cases, the cells were then rinsed with PBS and viewed with a Leica SP5 confocal microscope equipped with a 488 nm argon laser and a 633 nm helium neon laser. Both LysoTracker and MitroTracker were excited at 488 nm and monitored at 500−570 nm, while compounds **2** and **5** were excited at 633 nm and monitored at 640−700 nm. The images were digitized and analyzed using the Leica Application Suite Advanced Fluorescence. The subcellular localization of **2** and **5** was revealed by comparing the intracellular fluorescence images caused by the LysoTracker or MitoTracker and these dyes.

Flow Cytometric Studies. Approximately 6×10^5 HT29 cells in the medium (2 mL) were seeded on a 35 mm dish and incubated for 24 h at 37 °C under 5% CO_2. The cells were then treated with **2** or **5** at various concentrations and incubated under the same conditions for 2 h. The cells were then rinsed thrice with PBS and refilled with 100 μL of the culture medium before being illuminated at ambient temperature using a halogen-lamp light source as described above. After 24 h of incubation, the cells were rinsed with PBS and then harvested by 0.25% trypsin−EDTA (Invitrogen, 500 μL) for 5 min, followed by centrifugation at 2400 rpm for 3 min. The pellet was then washed again by PBS and then subject to centrifugation. The cells were suspended in 1 mL of binding buffer (10 mM HEPES, 140 mM NaCl, 25 mM $CaCl_2$, pH 7.4) containing annexin V-GFP (5 μL) and PI (2 μg mL^{-1}). After incubation in darkness for 15 min at room temperature, the signals of annexin V-GFP and PI were measured by a BD FACSCanto flow cytometer (Becton Dickinson) with 10^4 cells counted in each sample. Both annexin V-GFP and PI were excited by a 488 nm argon laser. The emitted fluorescence was monitored at 500−560 nm for annexin V-GFP and at >670 nm for PI. The data collected were analyzed by using WinMDI 2.9.

In Vivo Photodynamic Treatment. Male Balb/c nude mice (20−25 g) were obtained from the Laboratory Animal Services Centre at The Chinese University of Hong Kong. All animal experiments had been approved by the Animal Experimentation Ethics Committee of the University. The mice were kept under a pathogen-free condition with free access of food and water. HT29 cells (1×10^7 cells in 200 μL) were inoculated subcutaneously on the back of the mice. The length, width, and thickness of tumor were measured by a micrometer digital caliper (SCITOP Systems). The tumor volume (mm^3) was calculated by the following formula: tumor volume = $\pi \times$ (length $\times$ width $\times$ thickness)/6. Once the tumors were grown to the size of 80−100 mm^3, the mice were used for in vivo PDT. First, phthalocyanines **2** and **5** were dissolved in THF and EtOH, respectively, to give 2.5 mM solutions, which were diluted to appropriate concentrations with 5% Cremophor EL in PBS. Then 1 μmol of drug per kg body weight (in 200 μL) was intravenously injected into the tail vein of the tumor-bearing mice. After 24 h post-injection, the tumor was illuminated by a diode laser (Biolitec Ceralas) at 675 nm operated at 0.1 W. Illumination on a spot size of 1.0 cm^2 for 5 min led to a total fluence of 30 J cm^{-2}. The tumor sizes of the nude mice were monitored periodically for the next 13 days. The tumor volumes were compared with three groups of control mice, namely, (i) treated with drug but nonilluminated, (ii) illuminated but without drug treatment, and (iii) neither drug nor light treatment.

Plasma Enzyme Activity Assays. Thirteen days after the in vivo PDT, four groups of nude mice were anesthetized with an intraperitoneal injection of ketamine and xylazine cocktail solution (200 μL). The blood (0.5 mL) of the mice was obtained by intracardiac puncture. Heparin (Sigma, 1250 UPS units mL^{-1}, 0.1 mL) was added to prevent blood coagulation. The blood samples were centrifuged at 5000 rpm at room temperature for 5 min. Then the plasma was collected. The activities of the hepatic enzymes aspartate aminotransferase (AST) and alanine aminotransferase (ALT) were measured by commercially available standard kits (Stanbio). The plasma (50 μL) was added to 1 mL of the assay reagents. Then the enzyme activities were determined by monitoring the absorbance changes at 340 nm for 3 min.

Acknowledgment. This work was supported by a grant from the Research Grant Council of the Hong Kong Special Administrative Region, China (Project No. 402608), and a strategic investments scheme administered by The Chinese University of Hong Kong.

Supporting Information Available: Comparison of the rates of photooxidation of DPBF in DMF using **1**−**9** and ZnPc as the photosensitizers; absorption spectra of **1** and **2** in water; changes in the Q-band absorbance and fluorescence intensity with pH for **1**−**9** in citrate buffer solutions; intracellular fluorescence images of HT29 caused by **5**, LysoTracker, and MitoTracker; the activity levels of hepatic marker enzymes (AST and ALT) in the serum of the mice after PDT treatment with **2** or **5**, and those for the controls; and electronic absorption and photophysical data for **1**−**9** in water. This material is available free of charge via the Internet at http://pubs.acs.org.

References

(1) Dolmans, D. E. J. G. J.; Fukumura, D.; Jain, R. K. Photodynamic therapy for cancer. *Nat. Rev. Cancer* **2003**, *3*, 380–387.
(2) Brown, S. B.; Brown, E. A.; Walker, I. The present and future role of photodynamic therapy in cancer treatment. *Lancet Oncol.* **2004**, *5*, 497–508.
(3) Wilson, B. C.; Patterson, M. S. The physics, biophysics and technology of photodynamic therapy. *Phys. Med. Biol.* **2008**, *53*, R61–R109.
(4) Celli, J. P.; Spring, B. Q.; Rizvi, I.; Evans, C. L.; Samkoe, K. S.; Verma, S.; Pogue, B. W.; Hasan, T. Imaging and photodynamic therapy: mechanisms, monitoring, and optimization. *Chem. Rev.* **2010**, *110*, 2795–2838.
(5) Detty, M. R.; Gibson, S. L; Wagner, S. J. Current clinical and preclinical photosensitizers for use in photodynamic therapy. *J. Med. Chem.* **2004**, *47*, 3897–3915.
(6) Nyman, E. S.; Hynninen, P. H. Research advances in the use of tetrapyrrolic photosensitizers for photodynamic therapy. *J. Photochem. Photobiol., B* **2004**, *73*, 1–28.
(7) O'Connor, A. E.; Gallagher, W. M.; Byrne, A. T. Porphyrin and nonporphyrin photosensitizers in oncology: preclinical and clinical advances in photodynamic therapy. *Photochem. Photobiol.* **2009**, *85*, 1053–1074.
(8) Garland, M. J.; Cassidy, C. M.; Woolfson, D.; Donnelly, R. F. Designing photosensitizers for photodynamic therapy: strategies, challenges and promising developments. *Future Med. Chem.* **2009**, *1*, 667–691.
(9) Derycke, A. S. L.; de Witte, P. A. M. Liposomes for photodynamic therapy. *Adv. Drug Delivery Rev.* **2004**, *56*, 17–30.
(10) Bechet, D.; Couleaud, P.; Frochot, C.; Viriot, M.-L.; Guillemin, F.; Barberi-Heyob, M. Nanoparticles as vehicles for delivery of photodynamic therapy agents. *Trends Biotechnol.* **2008**, *26*, 612–621.
(11) Nishiyama, N.; Morimoto, Y.; Jang, W.-D.; Kataoka, K. Design and development of dendrimer photosensitizer-incorporated polymeric micelles for enhanced photodynamic therapy. *Adv. Drug Delivery Rev.* **2009**, *61*, 327–338.
(12) Couleaud, P.; Morosini, V.; Frochot, C.; Richeter, S.; Raehm, L.; Durand, J.-O. Silica-based nanoparticles for photodynamic therapy applications. *Nanoscale* **2010**, *2*, 1083–1095.
(13) Sharman, W. M.; van Lier, J. E.; Allen, C. M. Targeted photodynamic therapy via receptor mediated delivery systems. *Adv. Drug Delivery Rev.* **2004**, *56*, 53–76.
(14) Solban, N.; Rizvi, I.; Hasan, T. Targeted photodynamic therapy. *Lasers Surg. Med.* **2006**, *38*, 522–531.
(15) Verma, S.; Watt, G. M.; Mai, Z.; Hasan, T. Strategies for enhanced photodynamic therapy effects. *Photochem. Photobiol.* **2007**, *83*, 996–1005.
(16) Lo, P.-C.; Chen, J.; Stefflova, K.; Warren, M. S.; Navab, R.; Bandarchi, B.; Mullins, S.; Tsao, M.; Cheng, J. D.; Zheng, G. Photodynamic molecular beacon triggered by fibroblast activation protein on cancer-associated fibroblasts for diagnosis and treatment of epithelial cancers. *J. Med. Chem.* **2009**, *52*, 358–368.
(17) Lovell, J. F.; Liu, T. W. B.; Chen, J.; Zheng, G. Activatable photosensitizers for imaging and therapy. *Chem. Rev.* **2010**, *110*, 2839–2857.

(18) Agostinelli, E.; Marques, M. P. M.; Calheiros, R.; Gil, F. P. S. C.; Tempera, G.; Viceconte, N.; Battaglia, V.; Grancara, S.; Toninello, A. Polyamines: fundamental characters in chemistry and biology. *Amino Acids* **2010**, *38*, 393–403.

(19) Igarashi, K.; Kashiwagi, K. Modulation of cellular function by polyamines. *Int. J. Biochem. Cell Biol.* **2010**, *42*, 39–51.

(20) Seiler, N.; Delcros, J. G.; Moulinoux, J. P. Polyamine transport in mammalian cells. An update. *Int. J. Biochem. Cell Biol.* **1996**, *28*, 843–861.

(21) Casero, R. A., Jr.; Woster, P. M. Recent advances in the development of polyamine analogues as antitumor agents. *J. Med. Chem.* **2009**, *52*, 4551–4573.

(22) Senanayake, T.; Amunugama, H.; Boncher, T. D.; Casero, R. A., Jr.; Woster, P. M. Design of polyamine-based therapeutic agents: new targets and new directions. *Essays Biochem.* **2009**, *46*, 77–94.

(23) Holley, J. L.; Mather, A.; Wheelhouse, R. T.; Cullis, P. M.; Hartley, J. A.; Bingham, J. P.; Cohen, G. M. Targeting of tumor cells and DNA by a chlorambucil spermidine conjugate. *Cancer Res.* **1992**, *52*, 4190–4195.

(24) Cullis, P. M.; Green, R. E.; Malone, M. E. Mechanism and reactivity of chlorambucil and chlorambucil−spermidine conjugate. *J. Chem. Soc., Perkin Trans. 2* **1995**, 1503–1511.

(25) Papadopoulou, M. V.; Rosenzweig, H. S.; Bloomer, W. D. Synthesis of a novel nitroimidazole-spermidine derivative as a tumor-targeted hypoxia-selective cytotoxin. *Bioorg. Med. Chem. Lett.* **2004**, *14*, 1519–1522.

(26) Yuan, Z.-M.; Egorin, M. J.; Rosen, D. M.; Simon, M. A.; Callery, P. S. Cellular pharmacology of N^1- and N^8-aziridinyl analogues of spermidine. *Cancer Res.* **1994**, *54*, 742–748.

(27) Eiseman, J. L.; Rogers, F. A.; Guo, Y.; Kauffman, J.; Sentz, D. L.; Klinger, M. F.; Callery, P. S.; Kyprianou, N. Tumor-targeted apoptosis by a novel spermine analogue, 1,12-diaziridinyl-4,9-diazadodecane, results in therapeutic efficacy and enhanced radiosensitivity of human prostate cancer. *Cancer Res.* **1998**, *58*, 4864–4870.

(28) Delcros, J.-G.; Tomasi, S.; Carrington, S.; Martin, B.; Renault, J.; Blagbrough, I. S.; Uriac, P. Effect of spermine conjugation on the cytotoxicity and cellular transport of acridine. *J. Med. Chem.* **2002**, *45*, 5098–5111.

(29) Battaglia, A.; Guerrini, A.; Baldelli, E.; Fontana, G.; Varchi, G.; Samori, C.; Bombardelli, E. Synthesis of 7- and 10-spermine conjugates of paclitaxel and 10-deacetyl-paclitaxel as potential prodrugs. *Tetrahedron Lett.* **2006**, *47*, 2667–2670.

(30) Dallavalle, S.; Giannini, G.; Alloatti, D.; Casati, A.; Marastoni, E.; Musso, L.; Merlini, L.; Morini, G.; Penco, S.; Pisano, C.; Tinelli, S.; De Cesare, M.; Beretta, G. L.; Zunino, F. Synthesis and cytotoxic activity of polyamine analogues of camptothecin. *J. Med. Chem.* **2006**, *49*, 5177–5186.

(31) Samor, C.; Guerrini, A.; Varchi, G.; Beretta, G. L.; Fontana, G.; Bombardelli, E.; Carenini, N.; Zunino, F.; Bertucci, C.; Fiori, J.; Battaglia, A. The role of polyamine architecture on the pharmacological activity of open lactone camptothecin−polyamine conjugates. *Bioconjugate Chem.* **2008**, *19*, 2270–2279.

(32) Lamarche, F.; Sol, V.; Huang, Y.-M.; Granet, R.; Guilloton, M.; Krausz, P. Synthesis and biological evaluation of polyamine−porphyrin conjugates as potential agents in photodynamic therapy (PDT). *J. Porphyrins Phthalocyanines* **2002**, *6*, 130–134.

(33) Sol, V.; Lamarche, F.; Enache, M.; Garcia, G.; Granet, R.; Guilloton, M.; Blais, J. C.; Krausz, P. Polyamine conjugates of meso-tritolylporphyrin and protoporphyrin IX: potential agents for photodynamic therapy of cancers. *Bioorg. Med. Chem.* **2006**, *14*, 1364–1377.

(34) Garcia, G.; Sol, V.; Lamarche, F.; Granet, R.; Guilloton, M.; Champavier, Y.; Krausz, P. Synthesis and photocytotoxic activity of new chlorin−polyamine conjugates. *Bioorg. Med. Chem. Lett.* **2006**, *16*, 3188–3192.

(35) Hahn, F.; Schmitz, K.; Balaban, T. S.; Bräse, S.; Schepers, U. Conjugation of spermine facilitates cellular uptake and enhances antitumor and antibiotic properties of highly lipophilic porphyrins. *ChemMedChem* **2008**, *3*, 1185–1188.

(36) Ménard, F.; Sol, V.; Ringot, C.; Granet, R.; Alves, S.; Le Morvan, C.; Queneau, Y.; Ono, N.; Krausz, P. Synthesis of tetraglucosyl- and tetrapolyamine-tetrabenzoporphyrin conjugates for an application in PDT. *Bioorg. Med. Chem.* **2009**, *17*, 7647–7657.

(37) Lo, P.-C.; Chan, C. M. H.; Liu, J.-Y.; Fong, W.-P.; Ng, D. K. P. Highly photocytotoxic glucosylated silicon(IV) phthalocyanines. Effects of peripheral chloro substitution on the photophysical and photodynamic properties. *J. Med. Chem.* **2007**, *50*, 2100–2107.

(38) Leung, S. C. H.; Lo, P.-C.; Ng, D. K. P.; Liu, W.-K.; Fung, K.-P.; Fong, W.-P. Photodynamic activity of BAM-SiPc, an unsymmetrical bisamino silicon(IV) phthalocyanine, in tumour-bearing nude mice. *Br. J. Pharmacol.* **2008**, *154*, 4–12.

(39) Liu, J.-Y.; Lo, P.-C.; Jiang, X.-J.; Fong, W.-P.; Ng, D. K. P. Synthesis and in vitro photodynamic activities of di-α-substituted zinc(II) phthalocyanine derivatives. *Dalton Trans.* **2009**, 4129–4135.

(40) Chan, C. M. H.; Lo, P.-C.; Yeung, S.-L.; Ng, D. K. P.; Fong, W.-P. Photodynamic activity of a glucoconjugated silicon(IV) phthalocyanine on human colon adenocarcinoma. *Cancer Biol. Ther.* **2010**, *10*, 126–134.

(41) Jiang, X.-J.; Lo, P.-C.; Tsang, Y.-M.; Yeung, S.-L.; Fong, W.-P.; Ng, D. K. P. Phthalocyanine−polyamine conjugates as pH-controlled photosensitizers for photodynamic therapy. *Chem.—Eur. J.* **2010**, *16*, 4777–4783.

(42) Jiang, X.-J.; Lo, P.-C.; Yeung, S.-L.; Fong, W.-P.; Ng, D. K. P. A pH-responsive fluorescence probe and photosensitizer based on a tetraamino silicon(IV) phthalocyanine. *Chem. Commun.* **2010**, *46*, 3188–3190.

(43) Karigiannis, G.; Papaioannou, D. Structure, biological activity and synthesis of polyamine analogues and conjugates. *Eur. J. Org. Chem.* **2000**, 1841–1863.

(44) Scalise, I.; Durantini, E. N. Synthesis, properties, and photodynamic inactivation of *Escherichia coli* using a cationic and a noncharged Zn(II) pyridyloxyphthalocyanine derivatives. *Bioorg. Med. Chem.* **2005**, *13*, 3037–3045.

(45) Lo, P.-C.; Huang, J.-D.; Cheng, D. Y. Y.; Chan, E. Y. M.; Fong, W.-P.; Ko, W.-H.; Ng, D. K. P. New amphiphilic silicon(IV) phthalocyanines as efficient photosensitizers for photodynamic therapy: synthesis, photophysical properties, and in vitro photodynamic activities. *Chem.—Eur. J.* **2004**, *10*, 4831–4838.

(46) Maree, M. D.; Kuznetsova, N.; Nyokong, T. Silicon octaphenoxyphthalocyanines: photostability and singlet oxygen quantum yields. *J. Photochem. Photobiol., A* **2001**, *140*, 117–125.

(47) Kaur, N.; Delcros, J.-G.; Martin, B.; Phanstiel, O., IV. Synthesis and biological evaluation of dihydromotuporamine derivatives in cells containing active polyamine transporters. *J. Med. Chem.* **2005**, *48*, 3832–3839.

(48) Hajri, A.; Wack, S.; Meyer, C.; Smith, M. K.; Leberquier, C.; Kedinger, M.; Aprahamian, M. In vitro and in vivo efficacy of Photofrin and pheophorbide *a*, a bacteriochlorin, in photodynamic therapy of colonic cancer cells. *Photochem. Photobiol.* **2002**, *75*, 140–148.

(49) Burns, M. R.; Carlson, C. L.; Vanderwerf, S. M.; Ziemer, J. R.; Weeks, R. S.; Cai, F.; Webb, H. K.; Graminski, G. F. Amino acid/spermine conjugates: polyamine amides as potent spermidine uptake inhibitors. *J. Med. Chem.* **2001**, *44*, 3632–3644.

(50) Wang, C.; Delcros, J.-G.; Biggerstaff, J.; Phanstiel, O., IV. Synthesis and biological evaluation of N^1-(anthracen-9-ylmethyl)triamines as molecular recognition elements for the polyamine transporter. *J. Med. Chem.* **2003**, *46*, 2663–2671.

(51) Oleinick, N. L.; Morris, R. L.; Belichenko, I. The role of apoptosis in response to photodynamic therapy: what, where, why, and how. *Photochem. Photobiol. Sci.* **2002**, *1*, 1–21.

(52) Vermes, I.; Haanen, C.; Steffens-Nakken, H.; Reutelingsperger, C. A novel assay for apoptosis. Flow cytometric detection of phosphatidylserine expression on early apoptotic cells using fluorescein labelled annexin V. *J Immunol. Methods.* **1995**, *184*, 39–51.

(53) Suzuki, T.; Moriya, M.; Sakamoto, T.; Suga, T.; Kishino, H.; Takahashi, H.; Ishikawa, M.; Nagai, K.; Imai, Y.; Sekino, E.; Ito, M.; Iwaasa, H.; Ishihara, A.; Tokita, S.; Kanatani, A.; Stato, N.; Fukami, T. Discovery of novel spiro-piperidine derivatives as highly potent and selective melanin-concentrating hormone 1 receptor antagonists. *Bioorg. Med. Chem. Lett.* **2009**, *19*, 3072–3077.

(54) Das, B.; Venkateswarlu, K.; Krishnaiah, M.; Holla, H. A highly chemoselective Boc protection of amines using sulfonic-acid-functionalized silica as an efficient heterogeneous recyclable catalyst. *Tetrahedron Lett.* **2006**, *47*, 7551–7556.

(55) Asaki, T.; Hamamoto, T.; Sugiyama, Y.; Kuwano, K.; Kuwabara, K. Structure−activity studies on diphenylpyrazine derivatives: a novel class of prostacyclin receptor agonists. *Bioorg. Med. Chem.* **2007**, *15*, 6692–6704.

(56) Eaton, D. F. Reference materials for fluorescence measurements. *Pure Appl. Chem.* **1988**, *60*, 1107–1114.

(57) Tada, H.; Shiho, O.; Kuroshima, K.; Koyama, M.; Tsukamoto, K. An improved colorimetric assay for interleukin-2. *J. Immunol. Methods* **1986**, *93*, 157–165.